

Dynamic social networks based on movement

Henry R. Scharf^{*1}, Mevin B. Hooten^{2, 1, 3}, Bailey K. Fosdick¹,
Devin S. Johnson⁴, Josh M. London⁴, and John W. Durban⁵

¹Department of Statistics, Colorado State University

²U.S. Geological Survey, Colorado Cooperative Fish and Wildlife Research Unit

³Department of Fish, Wildlife, and Conservation Biology, Colorado State University

⁴NOAA Alaska Fisheries Science Center

⁵NOAA Southwest Fisheries Science Center

April 5, 2024

Abstract

Network modeling techniques provide a means for quantifying social structure in populations of individuals. Data used to define social connectivity are often expensive to collect and based on case-specific, *ad hoc* criteria. Moreover, in applications involving animal social networks, collection of these data is often opportunistic and can be invasive. Frequently, the social network of interest for a given population is closely related to the way individuals move. Thus telemetry data, which are minimally-invasive and relatively inexpensive to collect, present an alternative source of information. We develop a framework for using telemetry data to infer social relationships among animals. To achieve this, we propose a Bayesian hierarchical model with an underlying dynamic social network controlling movement of individuals via two mechanisms: an attractive effect, and an aligning effect. We demonstrate the model and its ability to accurately identify complex social behavior in simulation, and apply our model to

This draft manuscript is distributed solely for purposes of scientific peer review. Its content is deliberative and predecisional, so it must not be disclosed or released by reviewers. Because the manuscript has not yet been approved for publication by the U.S. Geological Survey (USGS), it does not represent any official USGS finding or policy.

*Corresponding author: henry.scharf@colostate.edu

telemetry data arising from killer whales. Using auxiliary information about the study population, we investigate model validity and find the inferred dynamic social network is consistent with killer whale ecology and expert knowledge.

1 Introduction

Dynamic social networks are an important topic of study among ecologists for a variety of species and ecological processes (Pinter-Wollman et al. 2013, Krause et al. 2007, Croft et al. 2008, Wey et al. 2008, Sih et al. 2009). Social networks can help explain a myriad of behavioral activities in a population, including the characteristics of animal movement. Therefore, it is common to define social networks based on directly observable behavior such as the duration of time animals spend in close proximity to one another (e.g., African elephants *Loxodonta africana* Goldenberg et al. 2014), discrete counts of interactions (e.g., yellow (*Papio cynocephalus*) and anubis baboons (*Papio anubis*) Franz et al. 2015), or discrete counts of close encounters (e.g., barn swallows (*Hirundo rustica erythrogaster*) Levin et al. 2015). Challenges for researchers interested in studying animal social networks include expensive data collection procedures, and potential biases due to opportunistic observation.

Many species of marine mammals, and in particular killer whales (*Orcinus orca*), are complex and highly social creatures (Pitman and Durban 2012, Parsons et al. 2009, Williams and Lusseau 2006, Baird and Whitehead 2000). To better understand the behavior of killer whales, researchers wish to characterize their social relationships. Unfortunately, direct observation of killer whale interactions is challenging; it is not uncommon for individuals to travel 50km a day and to range over thousands of kilometers in a season (Durban and Pitman 2012, Andrews et al. 2008). Furthermore, observation of killer whales at close proximity has been found to significantly influence their movement behavior (Williams et al. 2002), which could directly effect measurements of social connectivity. In contrast, satellite tracking tags have been used to gather movement data for killer whales over several months (Durban and Pitman 2012, Andrews et al. 2008), and there is little evidence to suggest that tags alter behavior. Thus, a potential alternative to costly personal observations are telemetry data, which contain rich movement information at the individual level, and can be collected in remote areas at a

much lower cost.

The suite of models for animal telemetry data is vast and rapidly changing, including both continuous- and discrete-time approaches (see [McClintock et al. 2014](#) for a review). Yet there are only a few models that explicitly account for interactions among individuals in the population (e.g., [Russell et al. 2015](#), [Langrock et al. 2014](#), [Codling and Bode 2014](#), [Morales et al. 2010](#)). Moreover, methods are lacking that attempt to characterize pairwise connections between all members of the population. We propose a model for movement that incorporates plausible mechanistic effects on movement due to an underlying social network. Our model allows us to infer the specific characteristics of interaction in a given population and the underlying dynamic social network itself.

In our proposed discrete-time continuous-space model, we assume there exists an underlying (latent) dynamic social network among the individuals in the population. Conditional on the network characteristics and the positions of animals in the previous time step, the expected positions of individuals at the next time point are modeled jointly using a Gaussian Markov random field (GMRF) ([Besag 1974](#), [Besag and Kooperberg 1995](#), [Rue and Held 2005](#)). The model is temporally Markovian for both the animal positions and the social network. In our model, the underlying social structure influences movement through two channels: an attractive effect and an alignment effect. These channels of interaction allow us to model a wide variety of behaviors, and they have a precedent for use in the context of interaction behavior ([Lemasson et al. 2013](#)). The connection between the underlying social network and position is an example of a hidden Markov model (HMM). HMMs represent a flexible class of hierarchical models popular in analyses of wildlife data in which an observable process (in our case, position) is driven by an unobserved Markovian process (the underlying social network).

We introduce the details of our proposed method in [Section 2](#). We demonstrate and assess inference from the model with simulated data in [Section 3](#). In [Section 4](#), we analyze data for seven killer whales tagged concurrently near the coast of the Antarctic Peninsula. Within the tagged sample, there are three genetically distinct types of killer whale ([Pitman and Ensor 2003](#), [Morin et al. 2015](#)) characterized by their size, coloration, and diet. The spatial distributions for each type overlap, and while strong social interaction is typical within each type, there have been no observed social associations among animals of different types. We demonstrate that inferences from our method are consistent with this history of observation. Furthermore, we

find strong evidence for dynamic social connections forming and dissolving within each type, but no indication of connections between types. Finally, in Section 5 we discuss potential extensions for the model, including the incorporation of environmental covariates and approaches for mediating the large computational demands for the model when the study sample is large.

2 Methods

We propose new methodology based on a general hierarchical modeling framework that accommodates measurement, process, and parameter uncertainty (Berliner 1996). We introduce the GMRF that describes animal movement in Section 2.1 and describe our method for modeling the dynamic social network in Section 2.2. Then in Section 2.3, we detail how we account for the fact that telemetry data are typically measured at individual-specific, irregularly spaced times with error.

2.1 Position Process

A GMRF is a description of a Gaussian random vector where conditional dependence between elements is specified based on a neighborhood structure (Rue and Held 2005). For example, data occurring at regular intervals in time, or on a lattice in space, are often modeled with GMRFs because natural neighborhoods exist for each datum (e.g., the preceding measurement in time, or the four closest spatial locations). Thus, GMRFs present a natural mathematical structure for modeling trajectories of connected individuals, as they provide a way to model dependence between connected or “neighboring” individuals.

We expect that social structure among individuals will influence their movement with respect to one another. Let $\mu_i(t)$ denote the position of individual i at time t . Assuming we know the population social structure (i.e., which individuals are socially affiliated with which other individuals), we model the movements of all individuals simultaneously using a GMRF involving two social behavioral mechanisms: one related to attraction toward the mean position of connected individuals, and the other related to alignment, or movement parallel to the paths taken by connected individuals. Although our model is flexible enough to capture attraction or repulsion, as well as alignment or anti-alignment, in most cases we expect to infer

assortative relations whereby individuals that are socially connected move “together.” For this reason, we discuss movement of connected individuals as aligned and attractive.

Attraction and alignment mechanisms are critical features of the mean positions of each individual at regular synchronous time steps. Models for locations on regular intervals have been developed by several others, including Brillinger and Stewart [1998], Jonsen et al. [2005], and Forester et al. [2007]. We define the social relations in terms of a dynamic binary network $\mathbf{W}(t)$ indexed at times $t = 1, \dots, T$, where entry $w_{ij}(t) = 1$ indicates a connection between individuals i and j at time t and $w_{ij}(t) = 0$ indicates a lack thereof.

We specify a GMRF conditionally, from the perspective of a single individual at a given time. The mean position of each individual i at time t conditioned on all other individuals’ positions at time t (denoted $\boldsymbol{\mu}_{-i}(t)$) and all positions at the previous time $t-1$ ($\boldsymbol{\mu}(t-1)$) follows a normal distribution with mean

$$\mathbb{E}(\boldsymbol{\mu}_i(t) | \boldsymbol{\mu}_{-i}(t), \boldsymbol{\mu}(t-1), \mathbf{W}(t), \mathbf{W}(t-1), \alpha, \beta, \sigma^2, c) \equiv \boldsymbol{\mu}_i(t-1) + \underbrace{\beta \tilde{\boldsymbol{\mu}}_i(t-1)}_{\text{attraction}} + \underbrace{\sum_{j \neq i} \alpha \frac{w_{ij}(t)}{w_{i+}^c(t)} [\boldsymbol{\mu}_j(t) - (\boldsymbol{\mu}_j(t-1) + \beta \tilde{\boldsymbol{\mu}}_j(t-1))]}_{\text{alignment}} \quad (1)$$

and precision

$$\text{Prec}(\boldsymbol{\mu}_i(t) | \mathbf{W}(t), \sigma^2, c) \equiv \sigma^{-2} w_{i+}^c(t) \mathbf{I}_2. \quad (2)$$

Focusing on (1), we model the expected location of individual i is equal to the sum of three terms: the individual’s location in the previous time period, $\boldsymbol{\mu}_i(t-1)$; an attraction term capturing the tendency for the individual to move toward other individuals it is socially connected to; and an alignment term accounting for the fact that groups of interconnected individuals will move in the same general direction.

The term $\tilde{\boldsymbol{\mu}}_i(t)$ in the attraction component of (1) is a unit vector pointing from individual i ’s position $\boldsymbol{\mu}_i(t)$ to the mean position $\bar{\boldsymbol{\mu}}_i(t)$ of all the

individuals it is connected to in $\mathbf{W}(t)$ (i.e., its ego-network):

$$\bar{\boldsymbol{\mu}}_i(t) \equiv \sum_{j \neq i}^n \frac{w_{ij}(t)}{w_{i+}^c(t)} \boldsymbol{\mu}_j(t) \quad (3)$$

$$\tilde{\boldsymbol{\mu}}_i(t) \equiv \begin{cases} \frac{\bar{\boldsymbol{\mu}}_i(t) - \boldsymbol{\mu}_i(t)}{\|\bar{\boldsymbol{\mu}}_i(t) - \boldsymbol{\mu}_i(t)\|_2}, & \sum_{j \neq i} w_{ij}(t) > 0 \\ 0 & \sum_{j \neq i} w_{ij}(t) = 0. \end{cases} \quad (4)$$

The parameter β controls the strength of the attractive effect of a social connection. On average, individual i moves a distance β in the direction $\tilde{\boldsymbol{\mu}}_i(t)$ during each time step.

In the above expression, $w_{i+}^c(t)$ is the size of individual i 's ego-network at time t if the individual has at least one connection (i.e., $w_{i+}^c(t) = \sum_{j \neq i} w_{ij}(t)$), and equal to a constant $w_{i+}^c(t) = c > 0$ otherwise. We require c to be strictly positive so the precision in (2) is non-zero for unconnected individuals.

The alignment term in (1) quantifies the mean displacement in position from $t - 1$ to t for only those individuals that individual i is socially connected to, and after accounting for attraction. Although the sum is over all individuals j , the social network indicators $w_{ij}(t)$ eliminate the effects of an individual's direction if it is not connected to individual i . The parameter α controls the strength of the aligning effect, with 0 corresponding to no alignment, and $\alpha \rightarrow 1$ corresponding to perfect alignment. The case $\alpha = 1$ corresponds to an intrinsically defined covariance matrix. In this paper, we limit our consideration to $\alpha < 1$.

Finally, the expression for the precision in (2) has the property that individuals who are more socially connected (i.e., have larger ego-networks $w_{i+}^c(t)$) have larger precision. The proportional relationship between precision and $w_{i+}^c(t)$ is required for a valid GMRF, and aligns with our intuition that, conditioned on the position of all other individuals, the movement of an individual with few or no social connections is more difficult to predict than one that experiences strong attraction and alignment toward a large group of individuals. The parameter c can be thought of as the effective size of the ego-network for an unconnected individual with regard to precision.

The specification of the model in (1) and (2) properly defines a GMRF where the elements of the precision matrix at time t are

$$Q_{ij}(t) \equiv \begin{cases} -\alpha w_{ij}(t) \sigma^{-2} \mathbf{I}_2, & j \neq i \\ w_{i+}^c(t) \sigma^{-2} \mathbf{I}_2, & j = i. \end{cases} \quad (5)$$

Therefore, we can write the multivariate version of the model for $t = 2, \dots, T$ as

$$[\boldsymbol{\mu}(t)|\boldsymbol{\mu}(t-1), \boldsymbol{\theta}] \equiv \mathcal{N}(\boldsymbol{\mu}(t-1) + \beta \tilde{\boldsymbol{\mu}}(t-1), \mathbf{Q}(t)), \quad (6)$$

where we have concatenated the model parameters $(\alpha, \beta, p_1, \phi, \sigma^2, c, \mathbf{W})$ into a single vector $\boldsymbol{\theta}$.

Notice that for the joint distribution in (6), the attraction effect remains in the mean structure because the attraction force for an individual is toward the previous location of the individuals in the ego-network. However, the alignment effects are encapsulated in the precision matrix because alignment is characterized by simultaneous movement of grouped individuals in the same direction. Figure 1 shows a schematic of the alignment and attraction effects graphically.

The model for movement based on the normalized vector $\tilde{\boldsymbol{\mu}}_i(t)$, instead of $\bar{\boldsymbol{\mu}}_i(t) - \boldsymbol{\mu}(t)$, reflects a mechanistic understanding that attractive movement is often restricted by how far an animal can reasonably travel in a given time step. We assume the maximum distance an individual is capable of moving during one time step to be approximately constant. Thus, when the gap between an individual and the center of its ego-network is large compared to its step size, an animal feeling an attractive pull will appear to take several steps of similar length in that direction.

If we used $\tilde{\boldsymbol{\mu}}(t)$ instead of the difference $\bar{\boldsymbol{\mu}}_i(t) - \boldsymbol{\mu}(t)$ in the attraction component of (1), the attractive pull an individual experienced when its ego-network was far away could be far greater than the distance it was able to travel in a single time step. To see this, note that the interpretation of β in (6) would change to reflect the average proportion of the gap between an individual and the center of its ego-network covered during each time step. A value of $\beta = 0.5$ would imply that an animal closes half the distance between itself and the center of its ego-network, regardless of the size of that gap. In some cases, the proportional gap coverage model may be more appropriate. In our application with killer whales, it is reasonable for connections between animals to form across relatively large gaps in space relative to the distance an animal might be able to cover in a single time step. Thus, the former interpretation is the most appropriate for our application.

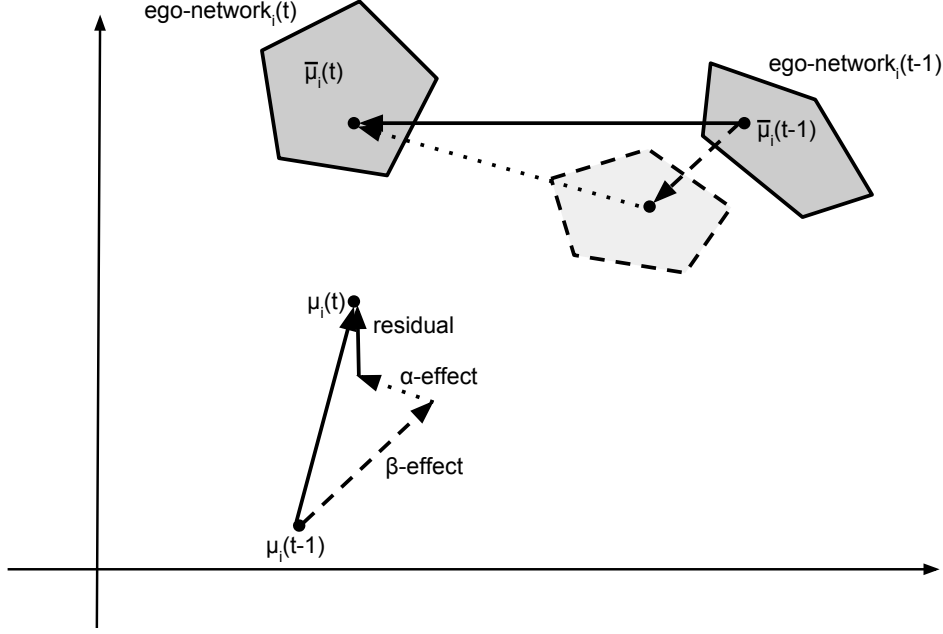


Figure 1: This schematic illustrates the two channels through which the dynamic social network influences movement. The dashed lines represent where the ego-network of individual i would be expected to be at time t under attraction alone, and the parallel dotted lines represent the alignment between individual i and the average of the differences $\boldsymbol{\mu}_j(t) - (\boldsymbol{\mu}_j(t-1) + \beta \tilde{\boldsymbol{\mu}}_j(t-1))$.

2.2 Dynamic Social Network

We model the dynamic process that gives rise to $\mathbf{W}(t)$ as a collection of pairwise independent Bernoulli random variables with a Markovian dependence in time, where

$$w_{ij}(1) \sim \text{Bern}(p_1) \quad (7)$$

$$w_{ij}(t) \sim \begin{cases} \text{Bern}(p_{1|0}), & w_{ij}(t-1) = 0 \\ \text{Bern}(p_{1|1}), & w_{ij}(t-1) = 1 \end{cases} \quad t = 2, \dots, T. \quad (8)$$

The parameter p_1 is the probability of a social connection between any two individuals at time $t = 1$, $p_{1|0}$ is the probability a pair of individuals who are

not connected at $t - 1$ become connected at time t , and $p_{1|1}$ is the conditional probability that a pair connected at time $t - 1$ remains connected at time t . Our model for $\boldsymbol{\mu}$ can thus be thought of as a HMM, where the latent social network \mathbf{W} takes on the role of the hidden Markovian process driving the observable position process.

Note that the expected proportion of possible edges that exist in the network (what we call network density) at time 1 is $\mathbb{E}(\mathbf{W}(1))/\binom{n}{2} = p_1$. Except for special cases of $p_{1|0}$ and $p_{1|1}$ (and implicitly defined $p_{0|0}$, and $p_{0|1}$), simulating from the model will yield a network whose density may grow or decay appreciably over time. While such a feature is not inherently a problem for network modeling, it may often be the case that the expected density of the social network should remain approximately constant over the period of study. However, it is not immediately clear what values of $p_{0|1}$ and $p_{1|1}$ generate such dynamic networks. By reparameterizing $p_{0|1}$ and $p_{1|1}$ in terms of a constant expected network density, p_1 , and a stability parameter, ϕ , we achieve a formulation of the model that is far more interpretable. Under our new parameterization, the edge probabilities can be written as

$$p_{1|0} = (1 - \phi)p_1, \quad p_{1|1} = 1 - (1 - \phi)(1 - p_1). \quad (9)$$

The above parameterization has the desirable property that the social network transitions from complete temporal independence to complete dependence (i.e., a static network) as the stability parameter ranges from 0 to 1. That is, $\lim_{\phi \rightarrow 0} p_{1|0} = \lim_{\phi \rightarrow 0} p_{0|1} = p_1$ and $\lim_{\phi \rightarrow 1} p_{1|0} = \lim_{\phi \rightarrow 1} p_{0|1} = 0$. Using the parameterization in (9) allows for simpler interpretation, and more straightforward solicitation of priors for Bayesian estimation. We provide additional details on this approach in Appendix A.

2.3 Measurement Error and Time Alignment

We will proceed with parameter estimation using Bayesian methodology. This motivates the top level of our hierarchical model, where we account for the fact that we do not typically measure $\boldsymbol{\mu}$ directly. Rather, we observe noisy measurements of position at asynchronous, irregularly occurring times. Let $\mathbf{s}_i(\tau_i)$ denote the observed position of individual i at time τ_i , and $[\mathbf{s}|\boldsymbol{\mu}, \boldsymbol{\theta}]$ the joint density of all individuals' observed locations conditioned on the mean underlying processes $\boldsymbol{\mu}$ and model parameters $\boldsymbol{\theta}$. To obtain inference for the parameters $\boldsymbol{\theta}$ given the observations \mathbf{s} (denoted $[\boldsymbol{\theta}|\mathbf{s}]$) using

standard Markov chain Monte Carlo (MCMC) methods would require that we specify a distribution for the measurement process $[\mathbf{s}|\boldsymbol{\mu}, \boldsymbol{\theta}]$. However, due to the temporal misalignment, it is difficult to specify a realistic parametric distribution. To address this problem, we make use of a multiple imputation procedure employed by [Hanks et al. \[2015, 2011\]](#), and [Hooten et al. \[2010\]](#), and a continuous-time correlated random walk model from [Johnson et al. \[2008\]](#). We outline the procedure briefly, and refer the reader to [Hanks et al. \[2011\]](#) and [Hooten et al. \[2010\]](#) for further details. Multiple imputation allows us to account for asynchronous, noisy position measurements while still permitting us to use a discrete-time, step-aligned structure for movement informed by a dynamic social network.

We have thus far constructed a model that provides inference for the posterior distribution of the model parameters $\boldsymbol{\theta}$ conditioned on the mean position process $\boldsymbol{\mu}$ ($[\boldsymbol{\theta}|\boldsymbol{\mu}]$). We are ultimately interested in the posterior distribution of $\boldsymbol{\theta}$ conditioned on the observed data. We could obtain the desired posterior distribution by evaluating the integral

$$[\boldsymbol{\theta}|\mathbf{s}] = \int [\boldsymbol{\theta}|\boldsymbol{\mu}] [\boldsymbol{\mu}|\mathbf{s}] d\boldsymbol{\mu}, \quad (10)$$

where we have assumed that the measurement process is independent of the movement process (that is, $[\mathbf{s}|\boldsymbol{\mu}, \boldsymbol{\theta}] = [\mathbf{s}|\boldsymbol{\mu}]$ and hence $[\boldsymbol{\theta}|\boldsymbol{\mu}, \mathbf{s}] = [\boldsymbol{\theta}|\boldsymbol{\mu}]$), but we do not have a closed form expression for $[\boldsymbol{\mu}|\mathbf{s}]$. However, using a process similar to $\boldsymbol{\mu}|\mathbf{s}$, which we denote $\boldsymbol{\mu}^*|\mathbf{s}$, we can approximate the integral in (10) via

$$[\boldsymbol{\theta}|\mathbf{s}] \approx \int [\boldsymbol{\theta}|\boldsymbol{\mu} = \boldsymbol{\mu}^*] [\boldsymbol{\mu}^*|\mathbf{s}] d\boldsymbol{\mu}^*. \quad (11)$$

If we are able to sample from $[\boldsymbol{\mu}^*|\mathbf{s}]$, we can evaluate the integral in (11) up to a constant of proportionality by drawing a realization from $[\boldsymbol{\mu}^*|\mathbf{s}]$ at every iteration of our MCMC algorithm, and updating model parameters $\boldsymbol{\theta}$ conditioned on the realization.

[Johnson et al. \[2008\]](#) introduced a continuous-time correlated random walk model that we use for $[\boldsymbol{\mu}^*|\mathbf{s}]$. The model relies on an Ornstein-Uhlenbeck process for velocity and observations of individuals paths that are conditionally independent (i.e., $[\mathbf{s}_i|\boldsymbol{\mu}^*] = [\mathbf{s}_i|\boldsymbol{\mu}_i^*]$). [Johnson et al. \[2011\]](#) provide an approach for sampling from the posterior predictive path $[\boldsymbol{\mu}_i^*|\mathbf{s}_i]$, which allows us to evaluate the integral in (11).

We can now obtain an approximation of our desired posterior by using the following two-step procedure:

1. Before initiating the Gibbs sampler, draw K different realizations from $[\boldsymbol{\mu}^*|\mathbf{s}]$ using the R package `crawl` (Johnson et al. 2008). In practice, a sufficiently large K in our application is on the order of 50.
2. At each iteration of the Gibbs sampler, draw one of the K samples and condition on this $\boldsymbol{\mu}^*$ for the updates.

3 Simulation

If our primary parameters of scientific interest are in the network \mathbf{W} , the natural way to evaluate the quality of our model is to focus attention on how well we are able to recover the network. A natural baseline model for comparison is one using only proximity as a criterion for social connectivity. We consider the proximity-based network defined by

$$W_{ij}^R(t) = I_{\|\boldsymbol{\mu}_i - \boldsymbol{\mu}_j\|_2 < R}. \quad (12)$$

Though it does not explicitly incorporate the behaviors of attraction and alignment, defining the network using (12) is computationally cheap and closely mirrors the way some data are collected in the field (Levin et al. 2015, Goldenberg et al. 2014). The proximity-based alternative therefore represents a viable alternative against which we can compare our model. However, failing to consider attraction and alignment effects can lead, for example, to spurious connections that arise when two unconnected individuals happen to pass each other by chance. Our simulation shows that our model is able to avoid such pitfalls.

In the following simulation, we generate directly from the proposed process model and fit the model using paths $\boldsymbol{\mu}$. Details of the methods we use to fit the model may be found in D. We use the posterior mode of \mathbf{W} as one estimate of the network, and use a variety of radii R with the proximity-based network, \mathbf{W}^R , to define a suite of alternatives. Because we know the true mean density of the network, p_1 , we select the proximity-based network for which the radius yields a mean density as close as possible to the true value. Choosing a radius that recovers the true mean density would not generally be possible, thus, we are comparing our model to a particularly favorable

proximity-based alternative. However, we still find that proximity alone provides a poor estimate of the true network relative to our proposed dynamic network model.

Figure 2 shows estimates of \mathbf{W} for a random selection of pairs. Included on each plot are the true network (green, solid), the posterior mean from the model fit (black, dashed), and the proximity-based estimate (dot-dashed, purple). We plot the posterior mean, rather than the mode, because it provides a visual intuition about uncertainty in our predicted network (e.g., posterior means of $w_{ij}(t)$ near 0.5 indicate large uncertainty in the mode). The individual pairs 3-4 and 1-6 show how the proximity-based network can both find spurious connections, and fail to identify connected behavior when it takes place over too large a distance. Table 1 shows 95% credible intervals for all parameters in the model except \mathbf{W} . All credible intervals capture the true parameter values, except those for ϕ . We observed moderate systematic bias in the posterior distribution of ϕ toward zero, however posterior inferences for \mathbf{W} were found to be robust in the presence of this bias. In most applications we expect the primary questions of scientific interest will surround the network \mathbf{W} , and ϕ can be treated as a nuisance parameter.

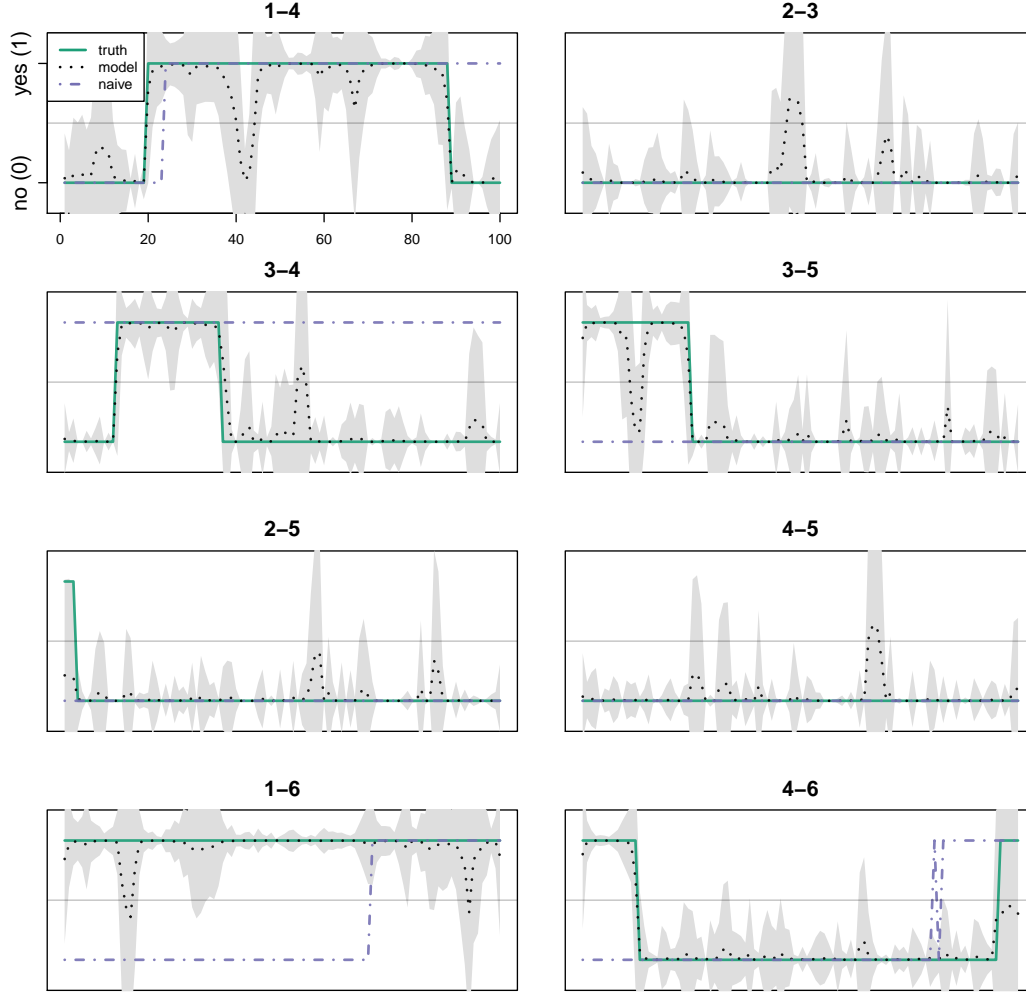


Figure 2: This figure shows a random subset of the complete estimated dynamic network for the simulated data on six individuals. The titles correspond to the i^{th} and j^{th} individuals in $w_{ij}(t)$. The solid green line is the true network, the black dotted line is the posterior mean from the proposed Bayesian hierarchical model, and the gray region represents one standard deviation above and below the posterior mean. The purple dot-dashed line is the network of individuals defined by \mathbf{W}^R , where individuals are deemed connected whenever they are separated by a distance less than R (see Section 3). R was chosen so that the mean density of the estimate network matched the true mean density p_1 .

parameter	true	median	(2.5%, 97.5%)
α	0.8	0.86	(0.79, 0.92)
β	0.5	0.49	(0.42, 0.57)
p_1	0.2	0.16	(0.10, 0.23)
ϕ	0.97	0.86	(0.76, 0.93)
c	0.33	0.29	(0.23, 0.36)
σ	1	0.95	(0.88, 1.03)

Table 1: This table shows marginal posterior medians and 95% credible intervals for model parameters. True values for the simulation were chosen to yield plausible movement paths.

Any study of a social network is ultimately based on a definition for connection specific to the population of interest. Thus, it would be incorrect to say that the proximity-based network fails to capture the true network. Rather, the proximity-based network simply does a poorer job describing the connections that influence movement than the network based on our proposed model. It is impossible to perfectly define a given social network, but if there is reason to believe that a study population might exhibit the commonly observed behaviors of attraction and alignment, then our model offers a way to study it. We have shown that ignoring these behaviors can result in misleading inference.

4 Killer whales

We analyze data gathered on seven individuals near the Antarctic Peninsula over the course of a week in February 2013 (for a description of the tags and study area see [Durban and Pitman 2012](#), [Andrews et al. 2008](#)). Geographic positions were measured using ARGOS transmitter tags. Within this area, three genetically distinct types of killer whales (termed A, B1, and B2) are known to exist ([Morin et al. 2015](#), [Pitman and Ensor 2003](#)) and are characterized primarily by their size, coloration, and diet. Type A killer whales are the largest and feed primarily on Antarctic minke whales (*Balaenoptera bonaerensis*) ([Pitman and Ensor 2003](#)). Of the two type B killer whales, B1 is larger and is distinguished by a diet consisting primarily of ice seals ([Durban and Pitman 2012](#)). Finally, type B2 killer whales are distinguished by an observed diet of penguins and likely fish during deep dives (personal

communication J. W. Durban 2015; [Pitman and Durban 2010](#)). Although all types of killer whales have been observed exhibiting social behavior within type, association between types has not been observed. The study sample of seven tagged whales consisted of three whales of Type A, one of type B1 and three of type B2.

Credible intervals for all parameters except the network \mathbf{W} are shown in Table 2. When we examine the mean step size across all individuals and times, we find it to be approximately 0.084, which is large compared to the contribution of attraction, suggesting only a moderate attractive effect. The fit also suggests a strong alignment effect evidenced by the posterior median for α falling close to 1. We therefore conclude that connectivity in this population of killer whales manifests itself predominantly as movement in parallel, with some additional tendency for connected individuals to move toward one another.

parameter	median	(2.5%, 97.5%)
α	0.87	(0.81, 0.92)
β	0.021	(0.015, 0.028)
p_1	0.12	(0.05, 0.21)
ϕ	0.95	(0.91, 0.97)
c	0.37	(0.25, 0.53)
σ	0.0036	(0.0027, 0.0048)

Table 2: This table shows marginal posterior medians and 95% credible intervals for model parameters when fit to the killer whale tagging data. The values reflect a strong alignment effect (α), weak attraction effect (β), and a stable (ϕ), sparse (p_1) social network.

The credible intervals for p_1 and ϕ suggest that the network is very stable, but also fairly sparse. Enduring connections are directly visible in Figure 3. The left column shows all pairwise dynamics between the three individuals of type B2, and the right column shows all pairwise dynamics between the three individuals of type A. All three individuals of type B2 show strong connection through the study period and, in fact all three of these individuals moved as a group during this time. The only social interaction involving individuals in type A occurred during the first few days of the study period between individuals 5 and 6. There was strong evidence for complete independence between all individuals not in the same type (see Figures B.1 and B.2 in the

appendix), consistent with expert knowledge. Of the 15 inter-type connections in \mathbf{W} , there were no posterior means above 0.5 at any time in the study period. A visualization of the movement and estimated social connections between these individuals can be found in [C](#).

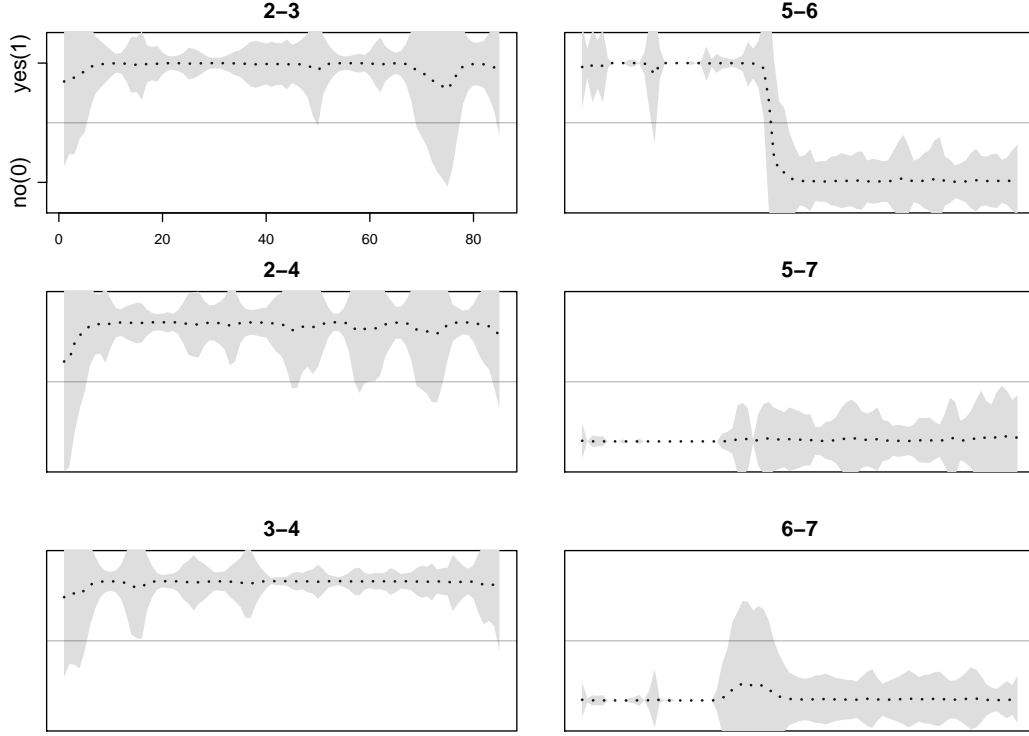


Figure 3: This figure shows a selection of the $\binom{7}{2} = 21$ possible pairs of individuals in the killer whale study sample. The left column is all pairs of killer whales of type B2 (labeled 2, 3, 4), and the right column is all pairs of killer whales of type A (labeled 5, 6, 7). Each plot shows the posterior mean for w_{ij} at all times t (dotted line) and one standard deviation above and below (gray region). No posterior means above 0.5 were predicted for inter-type connections.

5 Discussion

Existing methods for measuring and studying dynamic social networks in animal populations have several shortcomings. Namely, the methods are typically based on direct observation of the population of interest, which make the data expensive to collect. Additionally, the corresponding social network is defined based on *ad hoc* criteria determined by the researcher. It is natural to consider telemetry data as an alternative to direct observation, especially as these data become increasingly easy to collect. However, available models for animal movement do not generally incorporate interactions between individuals as drivers of movement, and those that do condition on a known dynamic social network. Spatio-temporal machine learning approaches have been proposed to detect patterns of movement such as flocking (e.g., [Zheng 2015](#), [Gudmundsson et al. 2004](#)), but these methods are primarily descriptive and do not offer measures of uncertainty, nor do they incorporate known scientific mechanisms. Our model addresses these limitations via a flexible, but interpretable, hierarchical framework that allows researchers to rigorously study dynamic social networks informed by relatively inexpensive telemetry data.

Moreover, our proposed model can easily be coupled with existing analyses on dynamic networks. Fundamentally, the study of dynamic social networks often begins with descriptive statistics such as network density, node degree, transitivity, and others ([Pinter-Wollman et al. 2013](#)). All of these common summaries can be obtained as derived quantities in our Bayesian framework along with estimates of uncertainty. More sophisticated models for dynamic networks (e.g., [Durante and Dunson 2014](#), [Sarkar and Moore 2005](#), [Sewell and Chen 2015](#)) can take the posterior mode of \mathbf{W} as input, or be incorporated as part of a larger hierarchical modeling structure.

We have shown, through simulation, that our proposed model is able to capture information about a population’s social network in a way that a simplistic proximity-based measure cannot, both by avoiding spurious connections and detecting interactions that occur over large distances. Through an application on killer whale movement, we have shown that the model captures connections consistent with expert knowledge based on non-quantitative observation, and can therefore be relied upon to deliver credible and practical inference.

When auxiliary covariates are available on the individuals, the proposed model can be extended to include such data. One approach to generalize

the model is to allow the spatial covariates to influence the mean position process of each individual, $\boldsymbol{\mu}_i(t)$, linearly. If we denote the matrix containing spatial covariates $\mathbf{X}_C(t)$, we arrive at a familiar additive form

$$[\boldsymbol{\mu}(t)|\boldsymbol{\mu}(t-1), \boldsymbol{\theta}, \boldsymbol{\gamma}] = \mathcal{N} \left(\underbrace{\mathbf{X}_C(t-1)\boldsymbol{\gamma}}_{\text{covariate effect}} + \underbrace{\mathbf{X}_W(t-1)\boldsymbol{\beta}}_{\text{attraction}}, \underbrace{\mathbf{Q}(t)}_{\text{alignment}} \right) \quad (13)$$

where

$$\mathbf{X}_W(t-1) \equiv [\boldsymbol{\mu}(t-1) \quad \tilde{\boldsymbol{\mu}}(t-1)], \quad \boldsymbol{\beta} \equiv \begin{bmatrix} 1 \\ \boldsymbol{\beta} \end{bmatrix}. \quad (14)$$

One limitation of our model is its ability to analyze large study samples in a reasonable amount of time. The number of parameters in our model grows at a rate of $\binom{n}{2}T$ as the number of individuals, n , and number of time points, T , increase. The most dominant factor in computation time will typically be n , and when the number of individuals grows beyond a few dozen, fitting the model on a laptop computer using MCMC becomes infeasible. One way to decrease the computational cost of fitting the model is to introduce additional structure on \mathbf{W} . We suggest two possible approaches.

The first way to introduce structure to \mathbf{W} is to define a maximum radius of interaction, R_{\max} , beyond which the probability of a social connection is zero. For example, the radius might be chosen to be the maximum distance at which two individuals are able to detect one another. After modifying the conditional distribution of $w_{ij}(t)$ based on R_{\max} , it is no longer necessary to update all $w_{ij}(t)$ in each step of the MCMC algorithm, only those for which $\|\boldsymbol{\mu}_i(t) - \boldsymbol{\mu}_j(t)\| < R_{\max}$. If R_{\max} is small relative to the spatial extent of the trajectories, this proximity-based modification offers a substantial reduction in the computational cost of fitting the model. This idea is somewhat related to covariance tapering for spatially referenced Gaussian random variables. [Furrer et al. \[2006\]](#) decrease the computational burden of interpolating, or kriging, by deliberately introducing zeros into the covariance matrix. In our setting, we would instead be introducing zeros into the precision matrix.

Another way to alleviate the computational burden would be to enforce structure directly on \mathbf{W} to reduce number of parameters in the model. For instance, it might be reasonable to assume that the social connections in a given population form as complete subgroups or cliques. In this case, the network describes a clustering process with only nT parameters. Though

motivated by straightforward mechanisms, both of these approaches to reducing the computational burden are non-trivial to implement. In the first case, setting a maximum radius of interaction complicates the enforcement of stability in the density of the network (introduced in Section 2.2) and offers modest or no gains when R_{\max} is large relative to the spatial extent of the individual paths. In the second case, updating the clustering process \mathbf{W} requires the exploration of a very large space (of cardinality equal to the Bell number B_n) for every t .

Although further developments are required before data for large populations of individuals can be accommodated, our framework provides a strong foundation for modeling relationships between movement and social networks.

6 Acknowledgments

Killer whale tagging was conducted under permit #14097 from the National Marine Fisheries Service and Antarctic Conservation Act permit #2009-013. Shipboard tagging operations were supported by Lindblad Expeditions and the National Geographic Society, and by an NSF rapid grant to Ari Friedlaender. Robert Pitman helped with tag deployments and identification of killer whale types in the field.

This research was supported by the NOAA and the National Marine Mammal Laboratory. Any use of trade, firm, or product names is for descriptive purposes only and does not imply endorsement by the U.S. Government.

References

- Russel D. Andrews, Robert L. Pitman, and Lisa T. Ballance. Satellite tracking reveals distinct movement patterns for type B and type C killer whales in the southern Ross Sea, Antarctica. *Polar Biology*, 31(12):1461–1468, November 2008.
- Robin W Baird and Hal Whitehead. Social organization of mammal-eating killer whales: group stability and dispersal patterns. *Canadian Journal of Zoology*, 78(12):2096–2105, December 2000.
- L. Mark Berliner. Hierarchical Bayesian time series models. In Kenneth M.

- Hanson and Richard N. Silver, editors, *Maximum Entropy and Bayesian Methods*, number 79 in Fundamental Theories of Physics, pages 15–22. Springer Netherlands, 1996.
- Julian Besag. Spatial interaction and the statistical analysis of lattice systems. *Journal of the Royal Statistical Society. Series B (Methodological)*, 36(2):192–236, January 1974.
- Julian Besag and Charles Kooperberg. On conditional and intrinsic autoregression. *Biometrika*, 82(4):733–746, December 1995.
- David R. Brillinger and Brent S. Stewart. Elephant-seal movements: Modelling migration. *Canadian Journal of Statistics*, 26(3):431–443, September 1998.
- Edward A. Codling and N. W. Bode. Copycat dynamics in leaderless animal group navigation. *Movement Ecology*, 2:11, 2014.
- Darren P. Croft, Richard James, and Jens Krause. *Exploring animal social networks*. Princeton University Press, July 2008.
- Daniele Durante and David B. Dunson. Nonparametric Bayes dynamic modeling of relational data. *Biometrika*, 101(4):883–898, 2014.
- J. W. Durban and R. L. Pitman. Antarctic killer whales make rapid, round-trip movements to subtropical waters: evidence for physiological maintenance migrations? *Biology Letters*, 8(2):274–277, April 2012.
- James D. Forester, Anthony R. Ives, Monica G. Turner, Dean P. Anderson, Daniel Fortin, Hawthorne L. Beyer, Douglas W. Smith, and Mark S. Boyce. State-space models link elk movement patterns to landscape characteristics in yellowstone national park. *Ecological Monographs*, 77(2):285–299, May 2007.
- Mathias Franz, Emily McLean, Jenny Tung, Jeanne Altmann, and Susan C. Alberts. Self-organizing dominance hierarchies in a wild primate population. *Proceedings of the Royal Society B: Biological Sciences*, 282(1814):20151512, September 2015.
- Reinhard Furrer, Marc G. Genton, and Douglas Nychka. Covariance tapering for interpolation of large spatial datasets. *Journal of Computational and Graphical Statistics*, 15(3):502–523, 2006.

- Shifra Z. Goldenberg, Shermin de Silva, Henrik B. Rasmussen, Iain Douglas-Hamilton, and George Wittemyer. Controlling for behavioural state reveals social dynamics among male African elephants, *loxodonta africana*. *Animal Behaviour*, 95:111–119, September 2014.
- Joachim Gudmundsson, Marc van Kreveld, and Bettina Speckmann. Efficient detection of motion patterns in spatio-temporal data sets. In *Proceedings of the 12th Annual ACM International Workshop on Geographic Information Systems*, GIS '04, pages 250–257, New York, NY, USA, 2004. ACM.
- Ephraim M. Hanks, Mevin B. Hooten, Devin S. Johnson, and Jeremy T. Sterling. Velocity-based movement modeling for individual and population level inference. *PLoS ONE*, 6(8)(8):e22795, August 2011.
- Ephraim M. Hanks, Erin M. Schliep, Mevin B. Hooten, and Jennifer A. Hoeting. Restricted spatial regression in practice: geostatistical models, confounding, and robustness under model misspecification. *Environmetrics*, 26(4):243–254, June 2015.
- Mevin B. Hooten, Devin S. Johnson, Ephraim M. Hanks, and John H. Lowry. Agent-based inference for animal movement and selection. *Journal of Agricultural, Biological, and Environmental Statistics*, 15(4):523–538, December 2010.
- Devin S. Johnson, Joshua M. London, Mary-Anne Lea, and John W. Durban. Continuous-time correlated random walk model for animal telemetry data. *Ecology*, 89(5):1208–1215, 2008.
- Devin S. Johnson, Josh M. London, and Carey E. Kuhn. Bayesian inference for animal space use and other movement metrics. *Journal of Agricultural, Biological, and Environmental Statistics*, 16(3):357–370, September 2011.
- Ian D. Jonsen, Joanna Mills Flemming, and Ransom A. Myers. Robust state-space modeling of animal movement data. *Ecology*, 86(11):2874–2880, November 2005.
- J. Krause, D. P. Croft, and R. James. Social network theory in the behavioural sciences: potential applications. *Behavioral Ecology and Sociobiology*, 62(1):15–27, October 2007.

- Roland Langrock, J. Grant C. Hopcraft, Paul G. Blackwell, Victoria Goodall, Ruth King, Mu Niu, Toby A. Patterson, Martin W. Pedersen, Anna Skarin, and Robert S. Schick. Modelling group dynamic animal movement. *Methods in Ecology and Evolution*, 5(2):190–199, 2014.
- B. H. Lemasson, J. J. Anderson, and R. A. Goodwin. Motion-guided attention promotes adaptive communications during social navigation. *Proceedings of the Royal Society B: Biological Sciences*, 280(1754):20122003, March 2013.
- Iris I. Levin, David M. Zonana, John M. Burt, and Rebecca J. Safran. Performance of Encounternet tags: field tests of miniaturized proximity loggers for use on small birds. *PLoS ONE*, 10(9):e0137242, September 2015.
- Brett T. McClintock, Devin S. Johnson, Mevin B. Hooten, Jay M. Ver Hoef, and Juan M. Morales. When to be discrete: the importance of time formulation in understanding animal movement. *Movement Ecology*, 2(1):21, October 2014.
- J. M. Morales, P. R. Moorcroft, J. Matthiopoulos, J. L. Frair, J. G. Kie, R. A. Powell, E. H. Merrill, and D. T. Haydon. Building the bridge between animal movement and population dynamics. *Philosophical Transactions of the Royal Society B: Biological Sciences*, 365(1550):2289–2301, July 2010.
- Phillip A Morin, Kim M Parsons, Frederick I Archer, María C Ávila-Arcos, Lance G Barrett-Lennard, Luciano Dalla Rosa, Sebastián Duchêne, John W Durban, Graeme M Ellis, Steven H Ferguson, John K Ford, Michael J Ford, Cristina Garilao, M Thomas P Gilbert, Kristin Kaschner, Craig O Matkin, Stephen D Petersen, Kelly M Robertson, Ingrid N Visser, Paul R Wade, Simon Y W Ho, and Andrew D Foote. Geographical and temporal dynamics of a global radiation and diversification in the killer whale. *Molecular ecology*, 24(15):3964–3979, 2015.
- K.M. Parsons, K.C. Balcomb, J.K.B. Ford, and J.W. Durban. The social dynamics of southern resident killer whales and conservation implications for this endangered population. *Animal Behaviour*, 77(4):963–971, 2009.
- Noa Pinter-Wollman, Elizabeth A. Hobson, Jennifer E. Smith, Andrew J. Edelman, Daizaburo Shizuka, Shermin de Silva, James S. Waters, Steven D. Prager, Takao Sasaki, George Wittemyer, Jennifer Fewell, and

- David B. McDonald. The dynamics of animal social networks: analytical, conceptual, and theoretical advances. *Behavioral Ecology*, page art047, June 2013.
- Robert L. Pitman and John W. Durban. Killer whale predation on penguins in Antarctica. *Polar Biology*, 33(11):1589–1594, 2010.
- Robert L. Pitman and John W. Durban. Cooperative hunting behavior, prey selectivity and prey handling by pack ice killer whales (*Orcinus orca*), type B, in Antarctic Peninsula waters. *Marine Mammal Science*, 28(1):16–36, 2012.
- Robert L. Pitman and Paul Ensor. Three forms of killer whales (*Orcinus orca*) in Antarctic waters. *Journal of Cetacean Research and Management*, 5(2):131–140, 2003.
- Havard Rue and Leonhard Held. *Gaussian Markov random fields: theory and applications*. CRC Press, February 2005.
- James C. Russell, Ephraim M. Hanks, and Murali Haran. Dynamic models of animal movement with spatial point process interactions. *Journal of Agricultural, Biological, and Environmental Statistics*, pages 1–19, September 2015.
- Purnamrita Sarkar and Andrew W. Moore. Dynamic social network analysis using latent space models. *SIGKDD Explor. Newsl.*, 7(2):31–40, December 2005.
- Daniel K. Sewell and Yuguo Chen. Latent space models for dynamic networks. *Journal of the American Statistical Association*, page (just accepted), January 2015.
- Andrew Sih, Sean F. Hanser, and Katherine A. McHugh. Social network theory: new insights and issues for behavioral ecologists. *Behavioral Ecology and Sociobiology*, 63(7):975–988, May 2009.
- Tina Wey, Daniel T. Blumstein, Weiwei Shen, and Ferenc Jordn. Social network analysis of animal behaviour: a promising tool for the study of sociality. *Animal Behaviour*, 75(2):333–344, February 2008.

- Rob Williams and David Lusseau. A killer whale social network is vulnerable to targeted removals. *Biology Letters*, 2(4):497–500, December 2006.
- Rob Williams, Andrew W. Trites, and David E. Bain. Behavioural responses of killer whales (*Orcinus orca*) to whale-watching boats: opportunistic observations and experimental approaches. *Journal of Zoology*, 256(02): 255–270, February 2002.
- Yu Zheng. Trajectory data mining: an overview. *ACM Transactions on Intelligent Systems and Technology*, 6(3):1–41, May 2015.

A Stationary network density

In our model statement, we make the plausible assumption that the probability of a connection between any two animals is the same for all pairs (see Section 2.2). That is, the marginal probability $\mathbb{P}(w_{ij}(t) = 1) = p_1(t)$ for all i, j . Often, it is reasonable to further assume that the density of our social network,

$$\rho(t) = \binom{n}{2}^{-1} \sum_{i < j} w_{ij}(t), \quad (15)$$

should remain approximately constant over time. With this added requirement, we can obtain a useful restriction on the conditional probabilities $p_{1|0}$ and $p_{1|1}$. We take the perspective of a discrete-time Markov process for the probability of an edge or non-edge at a given time. We then impose a stationarity requirement to yield a dynamic network in which expected density remains constant in time.

First, we form a transition matrix of conditional probabilities

$$\mathbf{M}_{t+1|t} \equiv \begin{pmatrix} p_{0|0} & p_{0|1} \\ p_{1|0} & p_{1|1} \end{pmatrix}. \quad (16)$$

We model the matrix as constant in time and therefore suppress the subscript on \mathbf{M} . We define the marginal probabilities of a non-edge and edge between any two nodes at time t as the vector

$$\mathbf{p}_t = \begin{pmatrix} 1 - p_1(t) \\ p_1(t) \end{pmatrix}. \quad (17)$$

The transition matrix propagates these probabilities through time via

$$\mathbf{p}_{t+1} = \mathbf{M}\mathbf{p}_t. \quad (18)$$

The expected density of the network at time t is

$$\mathbb{E}(\rho_t) = \binom{n}{2}^{-1} \sum_{i < j} \mathbb{E}(w_{ij}(t)), \quad (19)$$

and for our uniform network, all expectations in the sum are $p_1(t)$, thus

$$\mathbb{E}(\rho_t) = p_1(t). \quad (20)$$

Imposing a stationarity constraint on the expected density is equivalent to imposing it on $p_1(t)$, thus

$$\mathbb{E}(\rho_t) = p_1(t) \equiv p_1 \quad (21)$$

for all t . Written in terms of the transition matrix we have

$$\mathbf{p} = \mathbf{M}\mathbf{p}, \quad (22)$$

which implies the following relationship between our conditional probabilities

$$\frac{p_{1|0}}{1 - p_{1|1}} = \frac{p_1}{1 - p_1}. \quad (23)$$

The transition matrix is fixed up to a constant, which we introduce as a “stability” parameter ϕ . One can parameterize the stability of the network in several ways. We define

$$p_{1|0} \equiv (1 - \phi)p_1, \quad (24)$$

which forces

$$p_{0|1} = (1 - \phi)(1 - p_1) \quad (25)$$

$$p_{0|0} = 1 - (1 - \phi)p_1 \quad (26)$$

$$p_{1|1} = 1 - (1 - \phi)(1 - p_1). \quad (27)$$

B Dynamic social network between killer whale classes

B.1 Connections between killer whales: A - B2

Figure B.1 shows a selection of the $\binom{7}{2} = 21$ possible pairs of individuals in the killer whale study sample. The plots displayed are for all inter-type pairs of killer whales of type B2 (labeled 2, 3, 4) and A (labeled 5, 6, 7). Each plot shows the posterior mean for w_{ij} at all times t (dotted line) and one standard deviation above and below (gray region). No posterior means above 0.5 were predicted for inter-type connections. Combined with Figure B.2, we find strong evidence for independence between all three types.

http://www.stat.colostate.edu/~scharfh/supplemental/W_sample_COMPLETE1_2015_08_23_15:47:58_paper.pdf

B.2 Connections between killer whales: B1 - B2, A

Figure B.2 shows a selection of the $\binom{7}{2} = 21$ possible pairs of individuals in the killer whale study sample. The plots displayed are for all inter-type pairs of killer whales between the sole individual of type B1 (labeled 1) and those of type B2 (labeled 2, 3, 4) and A (labeled 5, 6, 7). Each plot shows the posterior mean for w_{ij} at all times t (dotted line) and one standard deviation above and below (gray region). No posterior means above 0.5 were predicted for inter-type connections. Combined with Figure B.1, we find strong evidence for independence between all three types.

http://www.stat.colostate.edu/~scharfh/supplemental/W_sample_COMPLETE2_2015_08_23_15:47:58_paper.pdf

C Animation of killer whales

http://www.stat.colostate.edu/~scharfh/anim/orca_nanim.html

D MCMC details

Priors and full-conditionals for the model are presented here.

http://www.stat.colostate.edu/~scharfh/supplemental/manuscript_supplement.pdf